

SUBMISSION TO GEOTECHNICAL TESTING JOURNAL

DATE:

Written 03 October 2017

TITLE:

A tensile strength apparatus with the facility to monitor negative pore-water pressure

AUTHORS:

Ian Murray*

Alessandro Tarantino **

Fernando Francescon ***

POSITION AND AFFILIATION:

* PhD student, Department of Civil and Environmental Engineering, University of Strathclyde

** Professor, Department of Civil and Environmental Engineering, University of Strathclyde

***MTP - Process Technology, Ideal Standard Italia S.r.l., Italy

CONTACT ADDRESS:

Professor Alessandro Tarantino

Department of Civil and Environmental Engineering

University of Strathclyde

James Weir Building - Level 5

75 Montrose Street - Glasgow G1 1XJ, Scotland, UK

E-mail: alessandro.tarantino@strath.ac.uk

KEYWORDS

Clay, cracking, failure, high-capacity tensiometer

I. Murray, A. Tarantino & F. Francescon

'A tensile strength apparatus with the facility to monitor negative pore-water pressure'

Submitted to Geotechnical Testing Journal

A TENSILE STRENGTH APPARATUS WITH THE FACILITY TO MONITOR NEGATIVE PORE-WATER PRESSURE

I. MURRAY, A. TARANTINO, AND F.FRANCESCON

ABSTRACT

This paper presents a new testing method for investigating the behaviour of clayey geomaterials subjected to a tensile (negative) total stress. The method includes the use of high capacity tensiometers to measure the pore-water pressure of the test specimen, an aspect which has not been demonstrated in any other direct tensile testing method. This addition allows interpretation of failure data in terms of effective stress rather than total stress, which is the approach that should be pursued in the saturated range. The test specimen shape and loading method have been modified from those commonly seen in existing literature to ensure that the direction of the major principal stress in the failure zone coincides with the direction of the externally applied tensile force, allowing for a more accurate analysis of tensile failure. Results are shown for saturated specimens and compared to results obtained for the same soil in uniaxial compression, using a modified version of the presented uniaxial tensile method, and a triaxial compression test. It is demonstrated that crack initiation occurs by shear failure if the data is interpreted in terms of effective stress rather than total stress, and that the failure mechanisms under tension do not differ from compression.

1. INTRODUCTION

When subjected to desiccation a soil will shrink. If this shrinkage is prevented tensile stresses will develop in the soil mass and cracking will occur. Fundamental to the understanding of desiccation cracking is an accurate understanding of the conditions which result in crack initiation. Determination of these conditions has, in the past, generally focused on a total stress based experimental procedure with little focus being put on the control or measurement of suction.

Tensile testing methods for soils can be divided into two categories based upon the method of load application; indirect tension tests and direct tension tests.

Indirect tests use a test specimen with a specifically designed geometry so that upon loading, either from a compressive force or bending moment, tensile stresses develop on a plane where specimen failure will eventually occur.

The Brazilian test, also referred to as the diametrical compression test or indirect tension test, has most commonly been used for testing concrete and rock, but has also been used for testing soils, see Frydman, 1964; Krishnayya and Eisenstein, 1974; Blazejczak, Horn and Pytka, 1995; Vilar et al., 2009; Stirling et al., 2015; Lin, Xiong and Yan, 2016; Akin and Likos, 2017. In this test, a cylindrical disk-shaped specimen, lying horizontally, is loaded with a compressive force through diametrically opposed rigid platens. There are no examples of suction measurement in the literature for the Brazilian test. Effective suction measurement would be very difficult due to the non-homogeneous stress field that develops during testing.

The flexure bending test is used in materials engineering for rock and concrete testing. It consists of the specimen acting as a beam supported at each end and a point load applied at the midspan. Under this load the beam deflects, the largest tensile and compressive forces occurring in the extreme bottom and top fibres respectively. The value of these extreme

1
2
3
4
5 stresses is generally calculated assuming linear elastic behaviour of the clay. The use of
6
7 equipment to measure the development of strain across the beam offers an alternative and
8
9 more reliable method than the assumption of linear elasticity. Measurement of the strain field
10
11 has been achieved for this test by Ajaz and Parry (1975) and Thusyanthan et al. (2007).
12

13
14 Direct tension tests are generally performed by applying a uniaxial stress to one of the
15
16 boundaries of the test specimen, while the opposite boundary is constrained, with the
17
18 remaining boundaries free to deform. Direct tests are generally simpler than indirect tests
19
20 because, as the tensile force is applied directly, the relationship between stress and strength
21
22 can be obtained without the need for complex analysis. In general, the force can be applied to
23
24 the soil in two ways: either by using moulds designed to hold the specimen (friction based)
25
26 from which the load can be applied or by bonding the loading system directly to the
27
28 specimen.
29

30
31 The majority of friction based tests follow a similar design of both specimen and
32
33 apparatus. The specimen has a larger cross-sectional area at its ends than in the centre. A
34
35 specimen is prepared in two moulds which act to hold the specimen upon loading. The
36
37 moulds have converging sides which effectively hold the specimen by friction. One of the
38
39 moulds is fixed in position while the other remains free to move and is the part to which the
40
41 loading is applied. Loading can either be stress or strain controlled. Recent examples of this
42
43 general method of tensile testing for soils include Kim and Hwang (2003), Rodriguez et al.
44
45 (2007) and Trabelsi et al. (2012). Minor modifications to this idea have been made by Snyder
46
47 and Millar (1985) who used a figure of eight shaped mould and Nahlawi et al. (2004), who
48
49 used shear keys instead of converging sides to grip the sample during testing. Criticism of
50
51 friction based tests is associated with the gripping of the soil laterally, which is likely to create
52
53 shear stresses from the contact between the specimen and the mould. To assess tensile failure
54
55
56
57
58
59
60

effectively, one should avoid the introduction of shear stresses close to the location of specimen failure.

Examples of direct bonding are far less common, this is due to difficulties in finding a suitable method of bonding the specimen, which is often soft and wet, to the traction system. Farrell (1967) used Araldite, an epoxy based adhesive resin to secure brass end-plates to a cylindrical soil specimen, which was then loaded to failure. In order to achieve a successful adhesion, it was necessary for the ends of the soil specimen to be dried beforehand. Epoxy resin was also used by Heibroek et al. (2003) as the bonding agent. The results show that the specimens tested were all unsaturated. Tang and Graham (2000) presented a method for testing unsaturated soils in tension using 2 half cylindrical moulds. The specimen was fixed securely to the moulds using an epoxy paste adhesive, however, Nahlawi, et al. (2004) reported problems with this adhesive.

Despite the difficulties associated with direct bonding of the specimen to the loading system reported in the literature, in particular for saturated specimens, this type of test appears to be the ideal loading method where an accurate determination of tensile stress at failure is required.

This paper presents a method that represents a step change in direct tensile testing. Direct bonding has been chosen, with a new bonding system to allow testing samples in both saturated and unsaturated states. The system implements HCTs to monitor suction allowing interpretation in terms of effective stress. With the exception of Thusyanthan et al. (2007), there are no tests with measurement of suction using HCTs.

2. TESTING APPARTUSES

1.1 *Uniaxial tensile test apparatus*

The tensile test is designed as a direct test giving control over the applied axial total stress. The test is similar in concept to that developed at the Soil Mechanics laboratory at Polytechnic University of Catalonia (UPC) (Rodriguez, 2002), but has some significant modifications.

High capacity tensiometers (HCT), manufactured at Strathclyde University based upon the design by Tarantino and Mongiovi (2002), are used to measure the matric suction of the specimen throughout testing, allowing for an effective stress based analysis of the failure. Three tensiometers were used for each test. The tensiometers were placed onto the surface of the specimen, not embedded within it. One tensiometer was secured to each end of the sample and a third located in the centre section. The tensiometers at the ends of the specimen were held in place by the rigid restraints, while the centre tensiometer was held by a metal plate secured to the base of the apparatus. It is assumed that the tensiometer in the centre section did not influence the failure of the specimens as the location of failure was evenly distributed across the centre section. The suction measured by the centre tensiometer was used in the calculations as specimen failure always occurred in the centre section. The tensiometers at the end were used to validate the suction measured by the centre tensiometer.

The specimen is fixed using the adhesive at one end to a rigid restraint and at the opposite end to a rigid plate from which a hanger is attached via a low friction wheel. The ratio between the (horizontal) tensile force and the hanger dead weight was measured and found to be equal to 0.997. The specimen is placed on top of a layer of ball bearings to reduce frictional effects and allow the sample to deform freely during loading (Figure 1).

1.2 Uniaxial compression test apparatus

The uniaxial tensile apparatus was used as a method for testing specimens in compression. To do this a number of modifications to the tensile test apparatus were made. The applied loads required to reach failure in the sample were greater than those for the tensile test. To accommodate the increase in load the tensile test apparatus was mounted for convenience inside the tensile test apparatus of Rodriguez (2002) as shown in Figure 2. The low friction wheel, over which the load is applied was moved to be at the same end as the fixed mould. A loading system which bypasses the fixed mould and goes to the loading wheel was attached to the moveable mould. The metal plates used in the tensile test to restrain and load the specimen were fixed into position on the moveable and fixed mould. The test only used two tensiometers, located at the ends of the sample. A tensiometer in the centre section was tried but it was not possible to maintain a good connection between the tensiometer and the specimen (Figure 2).

3. DESIGN OF SPECIMEN SHAPE

Comsol Multiphysics, a finite element code, was used to assess and then optimise the shape of the test specimen. The soil was modelled as a linear elastic material (Young modulus $E = 205 \times 10^9 \text{ Pa}$, Poisson's ratio $\nu = 0.3$) and the analysis was performed assuming plane-strain conditions. The basic shape of samples used in friction based direct tests reported in the literature was considered as a starting point for the analysis. The centre section, with reduced area had to be sufficiently large as to allow the fixing of a tensiometer to the specimen, but was limited to 1.5cm due to the method of sample preparation. The centre section should also be of sufficient length to create an area where the stress state is homogeneous, but not so long as to make the specimens too flexible at higher water contents.

1
2
3
4
5 Figure 3 shows the deviator to isotropic stress ratio, q/p , for the sample with straight
6 sides, which is a similar geometry to Rodriguez (2002), where a deformation equivalent to an
7 average axial strain of 1% was applied at its end. It can be observed that the highest q/p values
8 occur at the transition between the centre section and the diagonals, which would trigger
9 failure at the transition corners rather than the sample centre.
10
11
12
13
14

15
16 The geometry was therefore modified by trial and error to eliminate the concentration of
17 deviator stresses at the transition corners. The values of q/p generated by the same
18 deformation in the sample with curved transition are shown in Figure 4, using the dimensions
19 of the shape finally adopted, shown in Figure 5. The highest q/p values now occur in the
20 centre section where the stress state appears to be reasonably homogeneous.
21
22
23
24
25
26
27

28 4. MATERIAL AND SPECIMEN PREPARATION

29
30 The material used in the tests for the results shown was a Vitreous China mix (ball clay,
31 Kaolin, quartz and feldspar), a material commonly used in the ceramic industry. Figure 6
32 shows the particle size distribution.
33
34
35
36

37 Specimens were prepared by slip casting in plaster moulds. The plaster has a high suction
38 which removes water from the liquid slip to form a plastic specimen. Plaster moulds were
39 used because they were able to produce specimens of complex shape in a relatively short
40 time.
41
42
43
44

45 The VC slip was obtained by mixing the different 'ingredients', each component being
46 added to influence the behaviour of the overall mix, making it suitable for use in the ceramics
47 industry for the production of sanitary ware products. To ensure consistent specimens a large
48 quantity of the VC slip was prepared prior to beginning the experimental programme by
49 mixing the dry powdered constitutive parts with demineralised water to a moisture content of
50
51
52
53
54
55
56
57
58
59
60

1
2
3
4
5 approximately 0.30. The mixed slip was then stored in an air tight container for the period of
6
7 the experiments. Individual specimens were prepared by taking a portion of the re-mixed slip
8
9 adding de-mineralised water to reach the required slip density for casting (1.84kg/l, $w \approx 0.35$).

10
11 Slip was added to the plaster mould. The time required to dry the VC slip was 90 min.
12
13 Upon removal from the mould the moisture content of the specimens was in the range 0.2-
14
15 0.21.
16
17

18 Specimens were air dried, where necessary, to target moisture content for the required
19
20 test, vacuum sealed and stored for 24 hours prior to testing to obtain an equilibrium in the
21
22 moisture content throughout the specimen.
23
24

25 26 5. SPECIMEN INSTALLATION 27

28 In an ideal test evaporation from the specimen would be completely prevented. In reality,
29
30 this was not possible due to the complex specimen shape and the need to attach the
31
32 tensiometers. Initially petroleum jelly was coated onto the specimens to reduce the
33
34 evaporation. While this did reduce evaporation, and was easy to apply, the water contents of
35
36 the specimens at failure appeared to not be consistent (water contents at failure lay above the
37
38 normal consolidation line in the isotropic stress-water content plane). The reason for this is
39
40 not understood as all the petroleum jelly was removed from the surface of the specimen
41
42 before weighing and placing in the oven. To overcome this difficulty paraffin film was used
43
44 in place of petroleum jelly. Due to the relatively complex shape of the sample it was not
45
46 possible to create a completely effective barrier using the paraffin film to prevent evaporation.
47
48 The paraffin film could reduce the base rate of evaporation sufficiently for the change in
49
50 suction to be less than 1kPa per minute. A single piece of paraffin film could not be stretched
51
52 over the sample as this could provide a load path for the applied tensile load and increase the
53
54
55
56
57
58
59
60

1
2
3
4
5 load at which the sample fails. To overcome this problem multiple pieces of unstretched
6
7 paraffin film were used and then silicone grease was used to seal the pieces of paraffin film to
8
9 each other. The grease did not come into contact with the sample.

10
11 The specimen was placed onto the ball bearings and glued to the end restraints. The
12
13 adhesive used throughout the testing to bond the specimen to the loading system was Hilti Hit
14
15 RE500, a bi component epoxy mortar designed for rebar connections and heavy anchoring.
16
17 The adhesive was able to restrain all of the different soil conditions tested, with suctions
18
19 ranging from 100kPa to a near dry sample. The maximum axial tensile stress applied through
20
21 the adhesive was approximately 130kN/m².

22
23
24 Care had to be taken to align the specimen correctly to the restraints and to remove all the
25
26 glue from the tensiometer holes in the restraints before it cured. During the curing process,
27
28 dummy tensiometers were inserted in the holes in the restraints to minimise evaporation. The
29
30 specimen and apparatus were then covered with an additional cling film to further reduce
31
32 evaporation. The specimen was then left overnight to allow the adhesive to cure.

33
34
35 During early testing, the majority of tests failed under loading at one of the soil-adhesive
36
37 boundaries. This was attributed to an inability of the paraffin film and cling film to adequately
38
39 prevent evaporation from the specimen. After a short time (approximately 6 hours) the
40
41 adhesive cured sufficiently to prevent the specimen shrinkage associated with the evaporation.
42
43 This resulted in an increase in deviatoric stress along the glue boundaries. Although this was
44
45 not sufficiently large to cause cracking before loading, the stress caused by the restrained
46
47 evaporation, in addition to the applied stress during testing was enough to cause failure at the
48
49 soil-adhesive boundary, rather than in the centre of the specimen. To overcome this issue the
50
51 specimen and attached apparatus, while the adhesive was curing, were covered with a plastic
52
53 box. The relative humidity of the air inside the box was raised by placing beakers of hot water
54
55
56
57
58
59
60

1
2
3
4
5 inside. With the introduction of this technique there were no more instances of sample failure
6
7 at the specimen-adhesive boundary.

8
9 After curing of the adhesive, the 3 tensiometers were placed onto the specimen and
10
11 secured in place. A small amount of soil paste was used to ensure a good contact between the
12
13 tensiometer and the specimen. The test was again covered with the box while the tensiometers
14
15 came into equilibrium with the specimen. Prior to loading, the box and film were removed
16
17 from the specimen for a period of one hour to obtain a base evaporation rate.
18
19

20 21 6. EXPERIMENTAL PROCEDURE 22

23 24 *Uniaxial tension test* 25

26
27 Specimens were tested at the loading rate of 1.96 N/min (≈ 7 kPa/min) until rupture
28
29 occurred. To verify that the response time of the tensiometers is adequate compared to the
30
31 loading rate, an additional tensile test at a higher nominal loading rate of 23.5 N/min
32
33 (approximately 84 kPa/min) was performed.
34
35

36 The result of this test is compared to a 1.96 N/min standard test with a similar initial
37
38 pore-water pressure as shown in Figure 7. The base evaporation rate for both load rates was
39
40 accounted for using the change in suction measured by the centre tensiometer for the one-hour
41
42 period before the start of loading. The change in pore water pressure associated with the
43
44 loading was similar for both load rates. The effective stress state at failure for the specimens
45
46 with faster load rate was also on the same failure envelope as the tests from the 1.96 N/min
47
48 load rate, indicating that the load rate used had no effect on the test. The 1.96 N/min rate was
49
50 then used for the tests as it allowed the operator easier control during loading and the base
51
52 evaporation rate was not considered to be negatively affecting the test results.
53
54
55
56
57
58
59
60

The determination of the axial stress at failure required the measurement of the cross-sectional area at the onset of rupture. Due to the centre tensiometer, it was not possible to measure the cross-sectional area of the centre section where the failures were occurring during the tests. The only measurement of size of the centre section possible was to measure the dimensions immediately after the sample had failed. The measurements were taken from a section of the centre section that was not in immediate proximity to the failure.

To relate the post failure cross-sectional area to the area immediately before failure, which is necessary for the accurate calculation of the stress state at failure, tests were performed with the centre tensiometer removed and manual measurements of the width and height of the specimen taken during loading. The area after failure was also measured, allowing for the calculation of the percentage change between the cross-sectional area after failure and immediately before failure. This test was performed at three different specimen moisture contents to create a best fit line relating the percentage area change to the final moisture content of the specimen. This best fit was used to calculate a cross-sectional area at the time of failure for the tests with the centre tensiometer in place, given the measurements of the area and the moisture content of the specimen after failure.

Figure 8 shows the correlation between the water content at failure and the percentage cross-sectional area increase after failure occurs. The percentage change in area ΔA , was calculated from the best fit line:

$$\Delta A = 48.82 \cdot w_f - 6.134 \quad [1]$$

The cross-sectional area of the sample immediately before failure (A_f) was therefore calculated as follows:

$$A_f = h_m \cdot w_m \cdot \left(100 - \left((44.82 \cdot w_f) - 6.134\right)\right) \quad [2]$$

where h_m and w_m are the measured height and width of the specimen after failure has occurred and w_f is the moisture content of the specimen at failure.

Uniaxial compression test

As there was no tensiometer in the centre section the loading procedure was altered to allow for the propagation of the change in suction to reach the tensiometers in the end section. The specimen was loaded in steps and the duration of each step was determined by the time taken for the tensiometer readings to stabilise following an increase in load, i.e. rate of change measured by the tensiometers matched that of rate recorded prior to loading (accounting for baseline evaporation). The load was applied in steps of 4.9, 9.8, or 19.6N and the time required for the pore-water pressure to equalise ranged between 12 and 30 min. As there was no centre tensiometer it was possible to measure the cross-sectional area of the centre section throughout the test with callipers.

A procedure similar to the uniaxial tensile test was adopted to glue the specimen to the loading ends and to install the tensiometers. The only exception was the use of petroleum jelly to cover the specimen during the curing stage. At the time of the compression test it was not yet known that the petroleum jelly was causing errors in measured water content.

Two specimens having initial water content of 0.197 and 0.185 respectively were tested. The specimen with initial moisture content of 0.197 was loaded in steps of 4.9N (≈ 15 kPa) with each load maintained for 12 minutes (sufficient to ensure pore-water pressure equilibration). The specimen with initial moisture content of 0.185 was loaded in steps of 19.6N (≈ 60 kPa) every 30 minutes until the stress conditions were equivalent to a friction angle of 20° , then in steps of 9.8N (≈ 30 kPa) until rupture. The increment in loading was

changed as the specimen approached failure to increase the precision of the applied load required to cause the specimen to rupture. Prior to each increase in load the dimension of the cross section of the centre section were measured with callipers. The test was considered to have failed correctly if the sample did not buckle in any direction prior to failure. After failure, a piece of the centre section was placed into the oven for 24hrs to obtain the moisture content.

7. RESULTS

Evolution of pore-water pressure during the test

The results of 3 uniaxial tensile tests are shown in this paper. Figure 9 shows the evolution of pore-water pressure for the specimen tested at $w=18.9\%$ ($p'_0=262\text{kPa}$). After the installation of the three tensiometers (two at the ends and one in the middle) the equilibrium was reached after about 200 minutes for the middle tensiometer, and 400 minutes for the fixed and load tensiometers. To minimise evaporation during this period water evaporation was prevented by using the paraffin film, cling film and plastic cover as described previously.

At $t\sim 970\text{mins}$, the cling film and the plastic cover were removed (leaving the paraffin film layer in place). A decrease in pore-water pressure was observed due to the disturbance of the specimen. After a short time, the pore-water pressure recorded by the tensiometers recovered and all 3 tensiometers recorded a similar rate of change of pore-water pressure (baseline evaporation). The specimen was finally subjected to a tensile uniaxial stress at $t\sim 1052\text{ min}$. The load and fixed tensiometers show consistent measurement and recorded a decrease in pore-water pressure upon tension. The middle tensiometer recorded a greater decrease in pore-water pressure, which has been seen in the majority of tests performed. The pore-water pressure recorded by the centre tensiometer was then used to quantify the changes

in isotropic effective stress during the tensile test, the other two tensiometers were used to validate the measurement of the centre tensiometer.

Figure 10 shows the evolution of pore water pressure recorded by the tensiometers for the uniaxial compression test shown in this paper. After installation, equilibrium between the 2 tensiometers and the specimen was reached after approximately 100 minutes. At approximately 160 minutes the plastic container and film were removed from the specimen, leaving the coating of petroleum jelly in place. The specimen was left for a further 60 minutes to obtain the baseline evaporation. The baseline evaporation in the uniaxial compression test was higher than that of the uniaxial tensile tests, due to the paraffin film layer being a more effective method of preventing evaporation. The specimen was then loaded as described in the previous section until rupture occurred. The pore water pressure recorded by the 2 tensiometers shows an increase in pore-water pressure immediately following an increase in load, followed by a subsequent decrease as the pressure equilibrates and returns to the baseline evaporation rate.

Critical state data

The effective mean stress, p' , versus deviator stress, q , paths for the 3 uniaxial tensile tests, the uniaxial compression tests and a standard CU triaxial compression test are shown in Figure 11. Where p' and q are calculated from the following, assuming triaxial conditions:

$$p' = \frac{\sigma'_a + (2\sigma'_r)}{3} \quad [3]$$

$$q = \sigma'_a - \sigma'_r \quad [4]$$

where σ'_a and σ'_r are the axial and radial effective stresses.

The deviator stress for the uniaxial tensile tests have been adjusted to allow them to be directly compared to the compression test data using Equation 5:

$$q = \frac{M_c}{M_e} (\sigma'_r - \sigma'_a) \quad [5]$$

where M_c and M_e are critical state soil parameters defining the gradient of the critical state line in compression and extension respectively in the $q:p'$ plane. M_c was calculated from the best fit critical state line of the compression tests and M_e was the $q:p'$ ratio from each of the individual uniaxial tests at failure.

It can be observed from Figure 11 that using Eq 5 the uniaxial tensile test specimens reach the failure envelope created by best fitting the compression test failure points. This failure envelope is associated with a friction angle, ϕ' , of 27.8° , which is linked to M_c from the following:

$$\sin \phi' = \frac{3M_c}{6 + M_c} \quad [6]$$

It can be observed from Figure 11 that the uniaxial tensile test specimens reach the failure envelope created by the compression tests. In the volumetric plane, the uniaxial compression specimen data point lies above the normal consolidation line for the soil. This fault has been attributed to use of petroleum jelly, as the same issue was recorded with early uniaxial tensile

1
2
3
4
5 tests and ceased when paraffin film was used as a covering instead of petroleum jelly. The
6
7 data points for the uniaxial tensile specimens are all on or close to the critical state line. The
8
9 critical state line was created from triaxial compression tests.
10

11 The consistency of the results for the uniaxial tensile tests specimens shown, in both the
12
13 p' - q and the volumetric plane, with respect to the compression tests act as validation for both
14
15 the testing apparatus and experimental procedure for the investigation of soil behaviour in
16
17 tension.
18
19

20 The water contents from the uniaxial tensile test taken immediately after rupture from the
21
22 centre and the two ends of the specimens from beside the specimen-adhesive boundary, are
23
24 shown in Figure 12. The results show that the water contents of the samples taken from the
25
26 centre section of the specimen, where the failures occurred, was lower than that of the end
27
28 sections at the adhesive-specimen boundary. Figure 9 shows the tensiometer response during
29
30 a test. The pore water pressure in the centre section decreased more than at the ends of the
31
32 specimen. This response was recorded in the majority of the specimens tested. Considering
33
34 this pore-water profile it would be expected that the lower pore water pressure in the centre
35
36 section would create a water flow from the ends to the centre, resulting in higher water
37
38 content in the centre.
39
40

41 As mentioned previously it was not possible to prevent all of the evaporation from the
42
43 specimen. In order to check whether the lower water content in the centre was due to this
44
45 evaporation a 'mock' test was performed. A specimen was installed as per normal procedure.
46
47 At the point where in a standard test the specimen would be loaded the specimen was left
48
49 unloaded for the period of time required to carry out a normal test. The water contents of the
50
51 specimen were then measured. The water contents for the three locations were within a small
52
53 range of each other. The change in water content can therefore be assumed to be due to the
54
55
56
57
58
59
60

effect of the negative total stress applied during testing.

To investigate the water content issue further the test was modelled via finite element method (GeoStudio) using the Modified Cam-Clay constitutive model. For reasons of symmetry only half of the specimen was modelled.

In this simulation, the specimen was initially subjected to a suction of 350kPa. The specimen was then subjected to a deviatoric stress by applying a constant rate of axial extension of 0.2mm per time step. The specimen was modelled as being fully undrained. The model boundary conditions and parameters before the deformation was applied are shown in Figure 13 and Table 1 respectively.

Figure 14 shows the stress path in the centre of the specimen, as well as the pore water pressure at intervals of height in the specimen for each time step. It can be seen from the figure that as shearing occurs the pore water pressure in the centre of the specimen increases significantly, while the pore water pressure at the ends of the specimen shows a small decrease. The difference in magnitude of the increase in the centre to the decrease in the ends can be attributed to the relative size of the sections.

The increase in pore water pressure in the centre of a specimen shown in Figure 14 would result in a flow of water from the centre of the specimen to its ends. Although the sample is globally undrained, local drainage may occur within the specimen. The Modified Cam-Clay simulation has therefore justified the water content profile found in the specimen at the end of testing.

8. CONCLUSIONS

This paper has presented a new apparatus for investigating the behaviour of clayey geomaterials subjected to a tensile (negative) total stress. A key feature of the apparatus is the

1
2
3
4
5 facility to monitor the negative pore-water pressure using high capacity tensiometers. This
6
7 allows interpretation of the failure data in terms of effective stress rather than total stress. The
8
9 specimen shape has been designed to ensure that the direction of the major principal stress in
10
11 the failure zone coincides with the direction of the externally applied tensile force, allowing
12
13 for a more accurate analysis of tensile failure. The loading rate has been validated by testing
14
15 specimens at a different loading rate and a simple method has been implemented to assess the
16
17 cross-sectional area of the specimen at failure.
18

19
20 Results are shown for saturated specimens and compared to results obtained for the same
21
22 soil in uniaxial compression, using a modified version of the presented uniaxial tensile
23
24 method, and a triaxial compression test. It is demonstrated that that crack initiation occurs by
25
26 shear failure if data are interpreted in terms of effective stress rather than total stress and that
27
28 the failure mechanisms under tension do not differ from compression.
29

30 31 32 ACKNOWLEDGEMENTS

33
34
35 The authors wish to thank Ideal Standard International for supporting the research as well as
36
37 Derek McNee for his help constructing the test apparatus.
38
39
40
41
42

43 44 45 REFERENCES

- 46 Ajaz, A. and Parry, R.H.G., "Stress-strain behaviour of two compacted clays in tension and in
47 compression," *Géotechnique*, Vol. 25, No. 3, 1975, pp. 495-512.
48 Akin, I.D. and Likos, W.J., "Brazilian Tensile Strength Testing of Compacted
49 Clay," *Geotechnical Testing Journal*, Vol. 40, No. 4, 2017, pp. 608-617.
50 Blazejczak, D., Horn, R., and Pytka, J., "Soil tensile strength as affected by time, water
51 content and bulk density," *Int. Agrophysics*, Vol. 9, No. 3, 1995, pp. 179-188.
52 De Souza Villar, L.F., De Campos, T.M.P., Azevedo, R.F., and Zornberg, J.G., "Tensile
53 strength changes under drying and its correlations with total and matric
54 suctions," *Proceedings of the 17th International Conference on Soil Mechanics and
55 Geotechnical Engineering: The Academia and Practice of Geotechnical
56
57
58
59
60*

I. Murray, A. Tarantino & F. Francescon

'A tensile strength apparatus with the facility to monitor negative pore-water pressure'

Submitted to *Geotechnical Testing Journal*

- 1
2
3
4
5 *Engineering*. Vol. 1, 2009, pp. 793-796.
- 6 Farrell, D.A., Geacem, E.L., and Larson, W.E., "The effect of water content on axial strain in a
7 loam soil under tension and compression," *Soil Science Society of America*
8 *Proceedings*, Vol. 31, No. 4, 1967, pp 445-450.
- 9 Frydman, S., "The applicability of the Brazilian (indirect tension) test of soils," *Aust.*
10 *J. Appl. Sci.*, Vol. 15, 1964, pp 335-343.
- 11 Heibroek, G., Zeh, R., and Witt, K.J., "Tensile strength of compacted clays," *In Proceedings*
12 *of the International Conference - From Experimental Evidence towards Numerical*
13 *Modelling of Unsaturated Soils*, Weimar, Germany, Schanz Ed., Vol. 1, 2003, pp.
14 395-412.
- 15 Jaeger, J.C., and Cook, N.G.W., 1969, "Fundamentals of Rock Mechanics," Methuen and Co
16 Ltd, London.
- 17 Kim, T.H., and Hwang, C., "Modelling of tensile strength on moist granular earth material at
18 low water content," *Engineering Geology*, Vol. 69, 2002, pp. 233-244.
- 19 Krishnayya, A.V.G., and Eisenstein, Z. "Brazilian tensile test for soils," *Can. Geotech. J.*,
20 Vol. 11, 1974, pp. 632-642.
- 21 Lin, H., Xiong, W., and Yan, Q., "Three-Dimensional Effect of Tensile Strength in the
22 Standard Brazilian Test Considering Contact Length," *Geotechnical Testing Journal*,
23 Vol. 39, No. 1, 2016, pp. 137-143.
- 24 Nahlawi, H., Chakrabarti, S., and Kodikara, J., "A direct tensile strength Testing Method for
25 unsaturated geomaterials," *Geotechnical Testing Journal*, Vol. 27, No. 4, 2004, pp.
26 356-361.
- 27 Rodriguez, R.L. 2002. Estudio experimentnal de flujo y transporte de cromo, niquel y
28 manganeso en residuos de la zona minera de Moa (Cuba): influencia del
29 comportamiento hidromecanico. Ph.D. thesis, Universitat Politecnica de Catalunya –
30 Barcelona Tech, Barcelona, Spain.
- 31 Rodriguez, R., Sanchez, M., Ledesma, A., and Lloret, A., "Experimental and numerical
32 analysis of desiccation of a mining waste". *Can Geotech J*, Vol. 44, No. 6, 2007, pp.
33 644-58.
- 34 Snyder, V.A. & Miller, R.D., "A pneumatic fracture method for measuring the tensile strength
35 of unsaturated soils", *Soil Science Society of America Journal*, Vol. 49, No. 6, 1985,
36 pp. 1369-1374.
- 37 Stirling, R.A., Hughes, P.N., Davie, C.T., and Glendinning, S., "Tensile behaviour of
38 unsaturated compacted clay soils - A direct assessment method", *Applied clay*
39 *science.*, Vol. 112-113, 2015, pp. 123-133.
- 40 Tang, G.X. and Graham, J., "A method for testing tensile strength in unsaturated soils",
41 *Geotechnical Testing Journal*, Vol. 23, No. 3, 2000, pp. 377-382.
- 42 Tarantino, A. and Mongiovi, L. 2002. Design and construction of a tensiometer for direct
43 measurement of matric suction. *Proceedings 3rd International Conference on*
44 *Unsaturated Soils*, pp. 319-324.
- 45 Thusyanthan, N.I., Take, W.A., Madabhushi, S.P.G., and Bolton, M.D., "Crack initiation in
46 clay observed in beam bending", *Geotechnique*, Vol. 57, No. 7, 2007, pp. 581-594.
- 47 Trabelsi, H., Jamei, M., Zenzri, H. and Olivella, S., "Crack patterns in clayey soils:
48 experiments and modelling", *Int J Numer Anal Meth Geomech*. Vol. 36, No. 11, 2011,
49 pp. 1410-1433.
- 50
51
52
53
54
55
56
57
58
59
60

1
2
3
4
5
6
7
8
9
10
11
12
13
14
15
16
17
18
19
20
21
22
23
24
25
26
27
28
29
30
31
32
33
34
35
36
37
38
39
40
41
42
43
44
45
46
47
48
49
50
51
52
53
54
55
56
57
58
59
60

For Review Only

1
2
3
4
5 **LIST OF CAPTIONS FOR TABLES**
6

7 Table 1 Parameters of Cam-clay model
8
9
10
11
12
13
14
15
16
17
18
19
20
21
22
23
24
25
26
27
28
29
30
31
32
33
34
35
36
37
38
39
40
41
42
43
44
45
46
47
48
49
50
51

52
53 **LIST OF CAPTIONS FOR ILLUSTRATIONS**
54

55 Figure 1 Uniaxial tensile test apparatus
56
57
58
59
60

For Review Only

1
2
3
4
5 Figure 2 Uniaxial compression apparatus

6
7 Figure 3 Stress state for uniaxial tensile specimen with straight sides

8
9 Figure 4 Stress state for uniaxial tension test specimen with curved sides

10
11 Figure 5 Dimensions of final specimen shape (mm)

12
13 Figure 6. Particle size distribution for Vitreous China

14
15 Figure 7 Comparison of uniaxial tension test load rate

16
17 Figure 8 Method for area correction for uniaxial tension test

18
19 Figure 9 Evolution of pre-water pressure recorded by the tensiometers in uniaxial tensile test

20
21 Figure 10 Evolution of pore-water pressure recorded by the tensiometers in the uniaxial compression
22
23 test

24
25 Figure 11 Critical state for uniaxial tension, uniaxial compression and triaxial compression test

26
27 Figure 12 Moisture content at different specimen locations at failure for uniaxial tension tests

28
29 Figure 13 Boundary conditions adopted in uniaxial test simulation

30
31 Figure 14 Results of uniaxial test simulation. (a) evolution of pore-water pressure with time. (b) stress
32
33 path in the p' - q plane
34
35

36
37
38 TABLES

39
40
41
42
43 Table 1 Parameters of Cam-clay model

44
45

Parameter	E (kPa)	ν	e_0	λ	κ	ϕ'	θ	K (m/sec)
Value	1000	0.334	0.353	0.0789	0.0132	20.84	0.5248	1e-8

46
47
48
49
50
51
52
53
54
55
56
57
58
59
60

I. Murray, A. Tarantino & F. Francescon

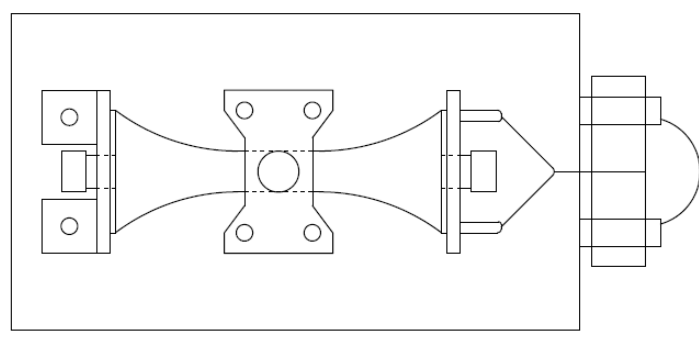
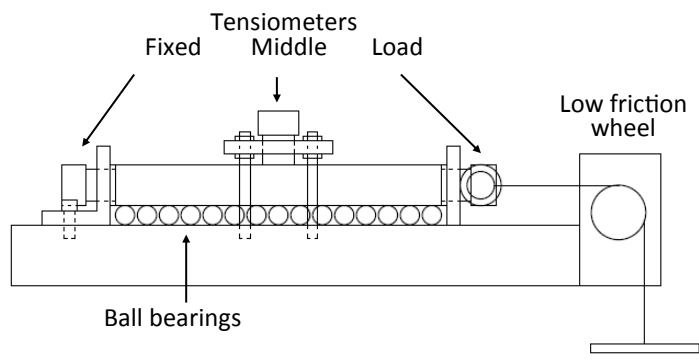
‘A tensile strength apparatus with the facility to monitor negative pore-water pressure’

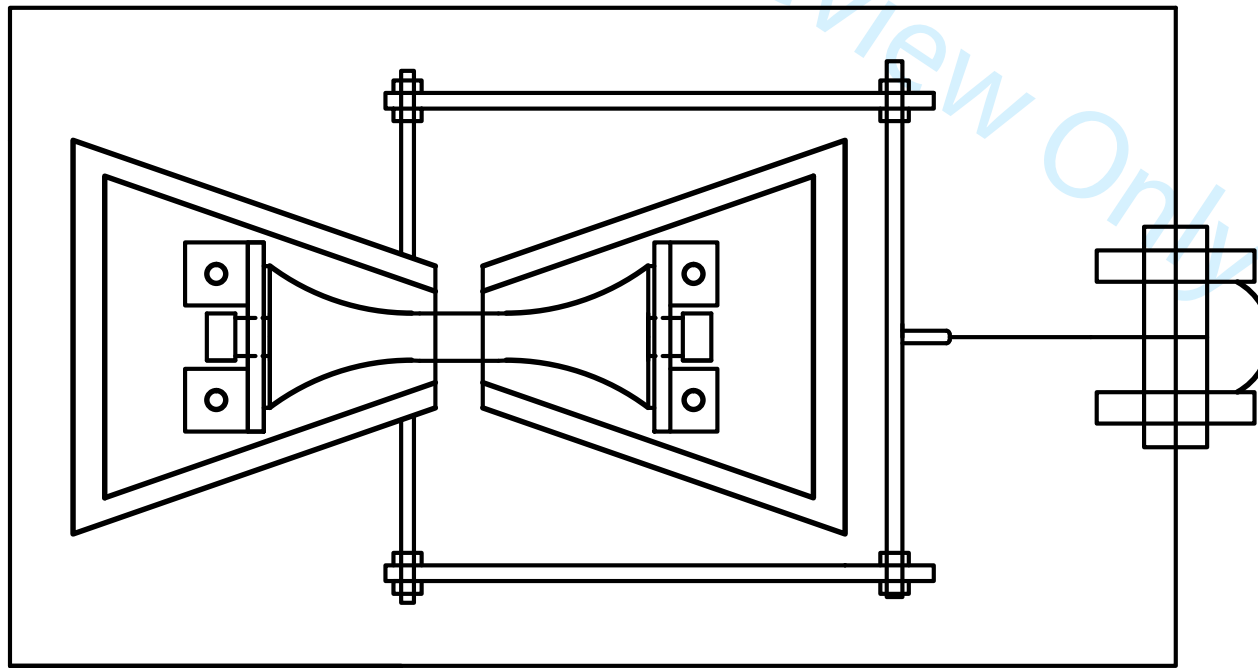
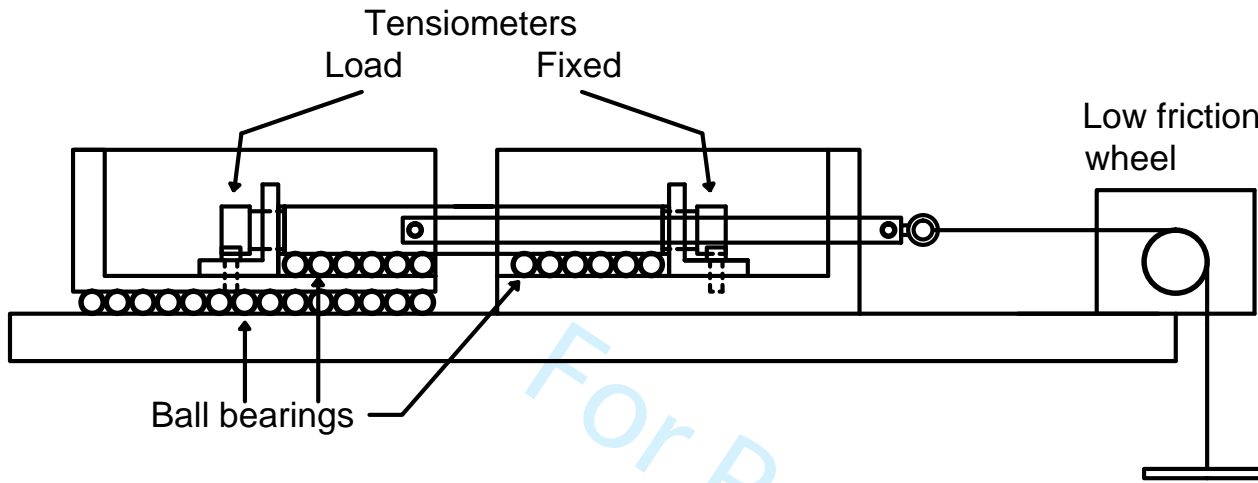
Submitted to Geotechnical Testing Journal

1
2
3
4
5
6
7
8
9
10
11
12
13
14
15
16
17
18
19
20
21
22
23
24
25
26
27
28
29
30
31
32
33
34
35
36
37
38
39
40
41
42
43
44
45
46
47
48
49
50
51
52
53
54
55
56
57
58
59
60

For Review Only

1
2
3
4
5
6
7
8
9
10
11
12
13
14
15
16
17
18
19
20
21
22
23
24
25
26
27
28
29
30
31
32
33
34
35
36
37
38
39
40
41
42
43
44
45
46
47
48
49
50
51
52
53
54
55
56
57
58
59
60





1
2
3
4
5
6
7
8
9
10
11
12
13
14
15
16
17
18
19
20
21
22
23
24
25
26
27
28
29
30
31
32
33
34
35
36
37
38
39
40
41
42
43
44
45
46

1
2
3
4
5
6
7
8
9
10
11
12
13
14
15
16
17
18
19
20
21
22
23
24
25
26
27
28
29
30
31
32
33
34
35
36
37
38
39
40
41
42
43
44
45
46
47
48
49
50
51
52
53
54
55
56
57
58
59
60

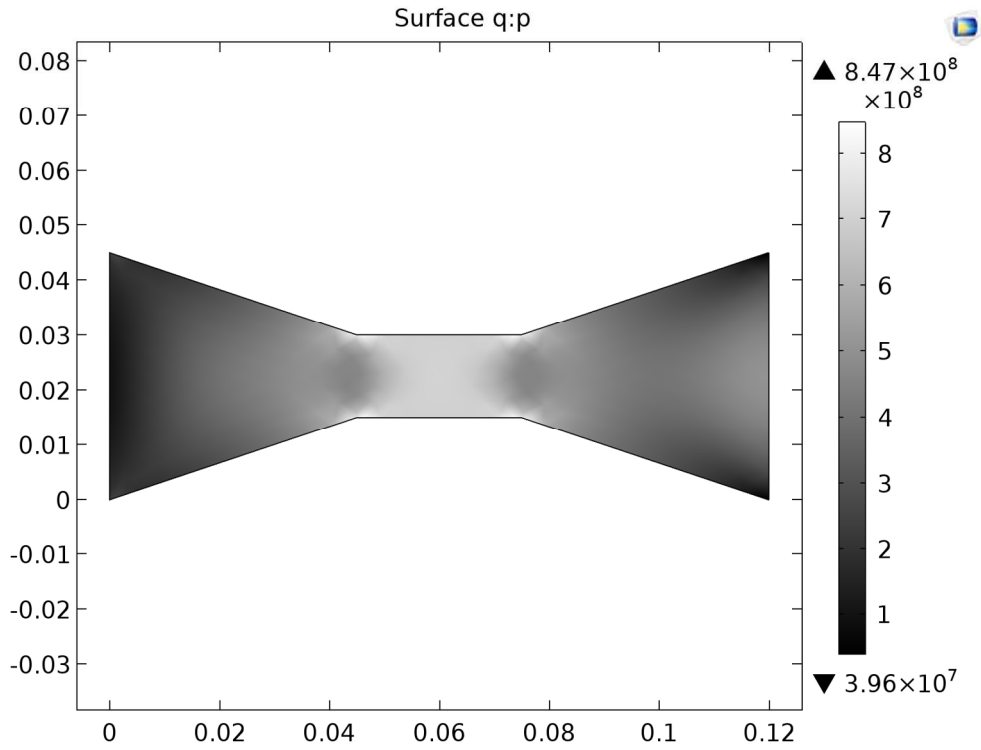


Figure 3 Stress state for uniaxial tensile specimen with straight sides
150x112mm (300 x 300 DPI)

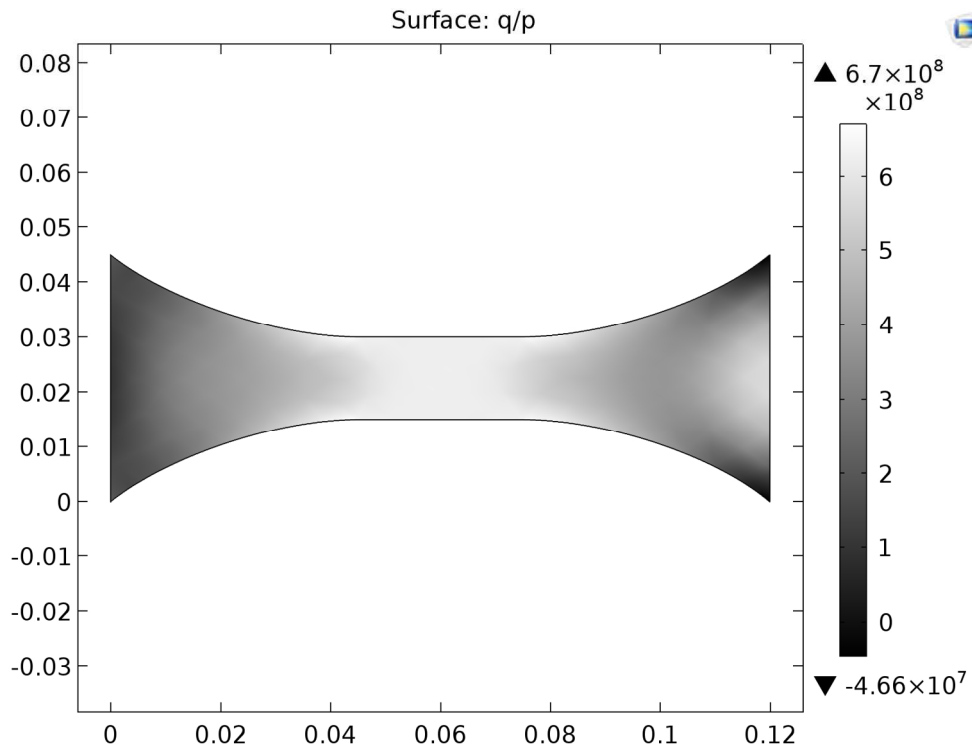
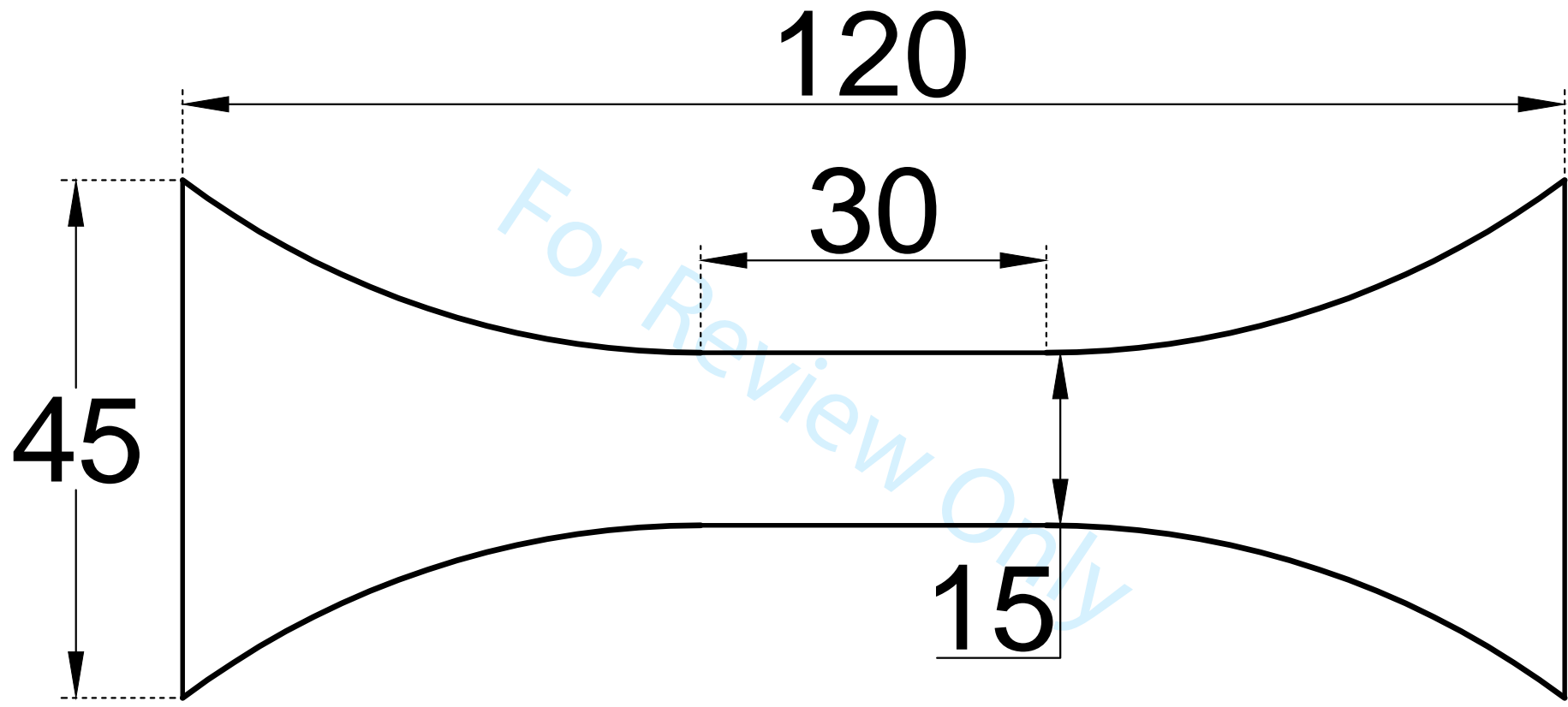


Figure 4 Stress state for uniaxial tensile specimen with curved sides

150x112mm (300 x 300 DPI)

Only



1
2
3
4
5
6
7
8
9
10
11
12
13
14
15
16
17
18
19
20
21
22
23
24
25
26
27
28
29
30
31
32
33
34
35
36
37
38
39
40
41
42
43
44
45
46

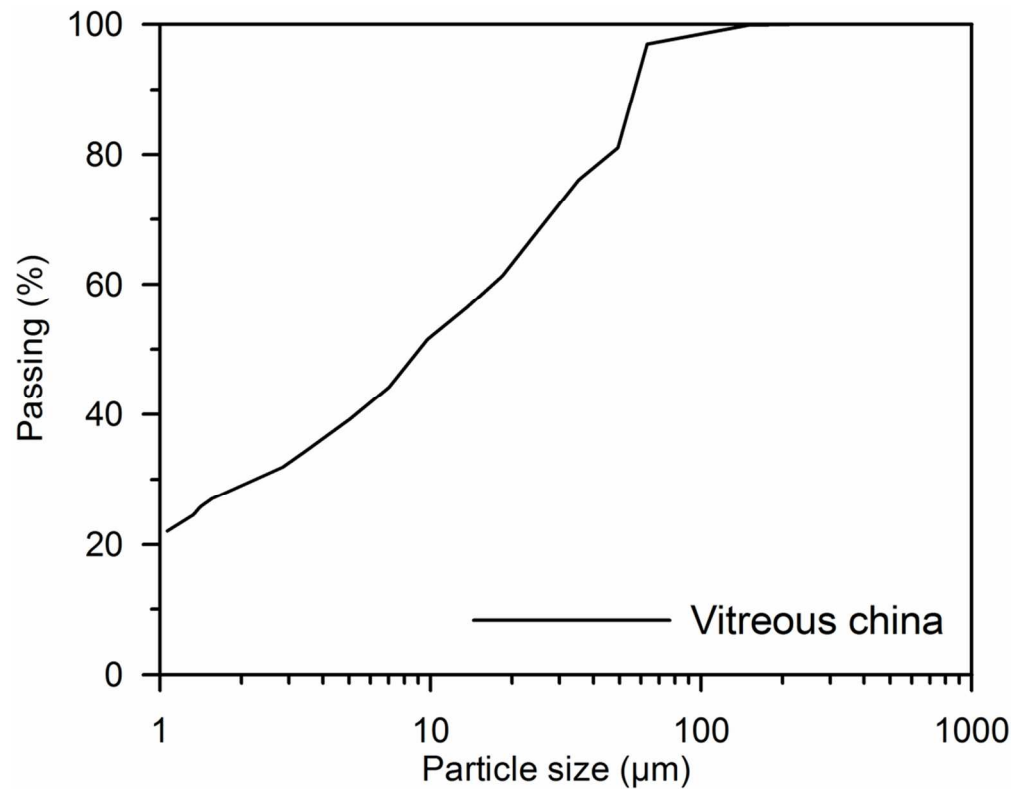


Figure 6. Particle size distribution for Vitreous China

96x75mm (300 x 300 DPI)

1
2
3
4
5
6
7
8
9
10
11
12
13
14
15
16
17
18
19
20
21
22
23
24
25
26
27
28
29
30
31
32
33
34
35
36
37
38
39
40
41
42
43
44
45
46
47
48
49
50
51
52
53
54
55
56
57
58
59
60

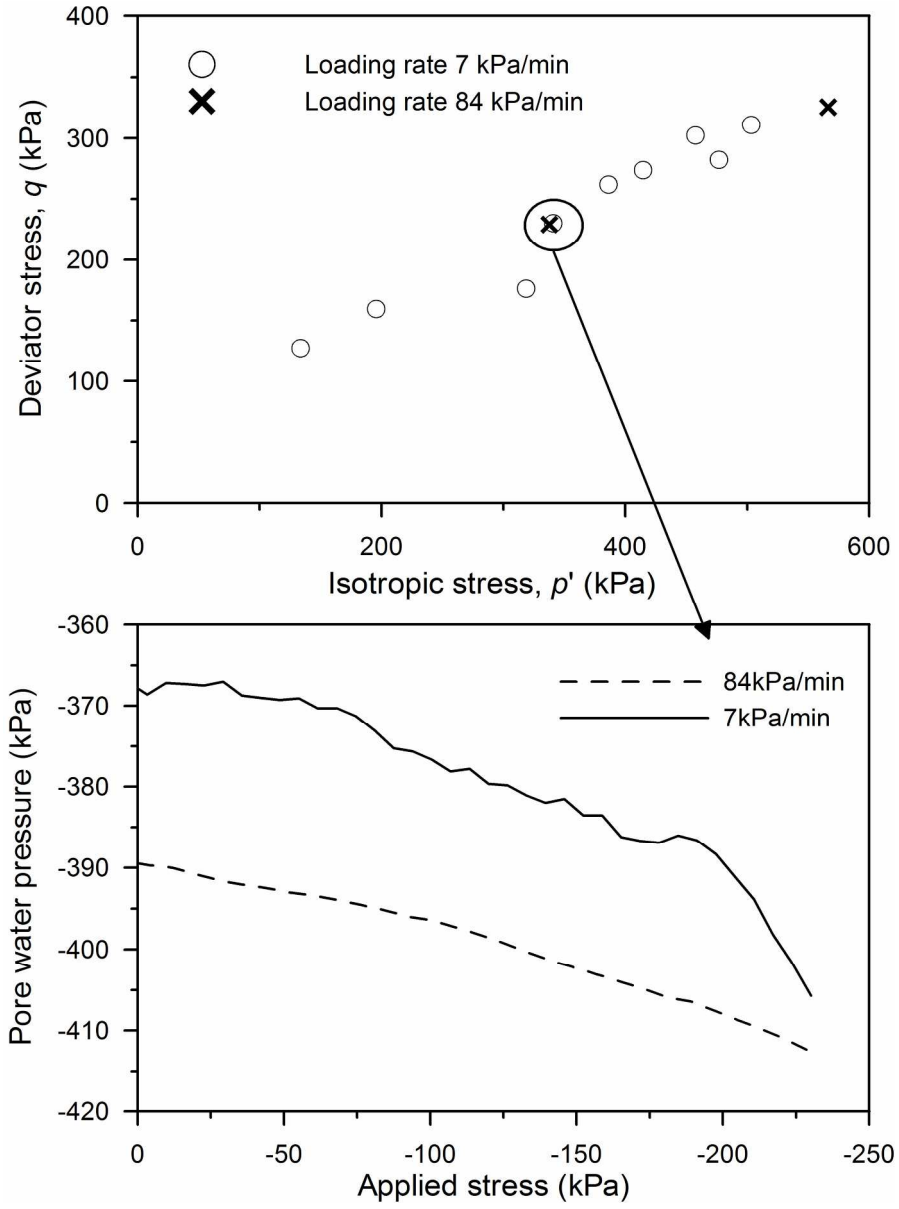


Figure 7 Comparison of uniaxial tension test load rate
197x265mm (300 x 300 DPI)

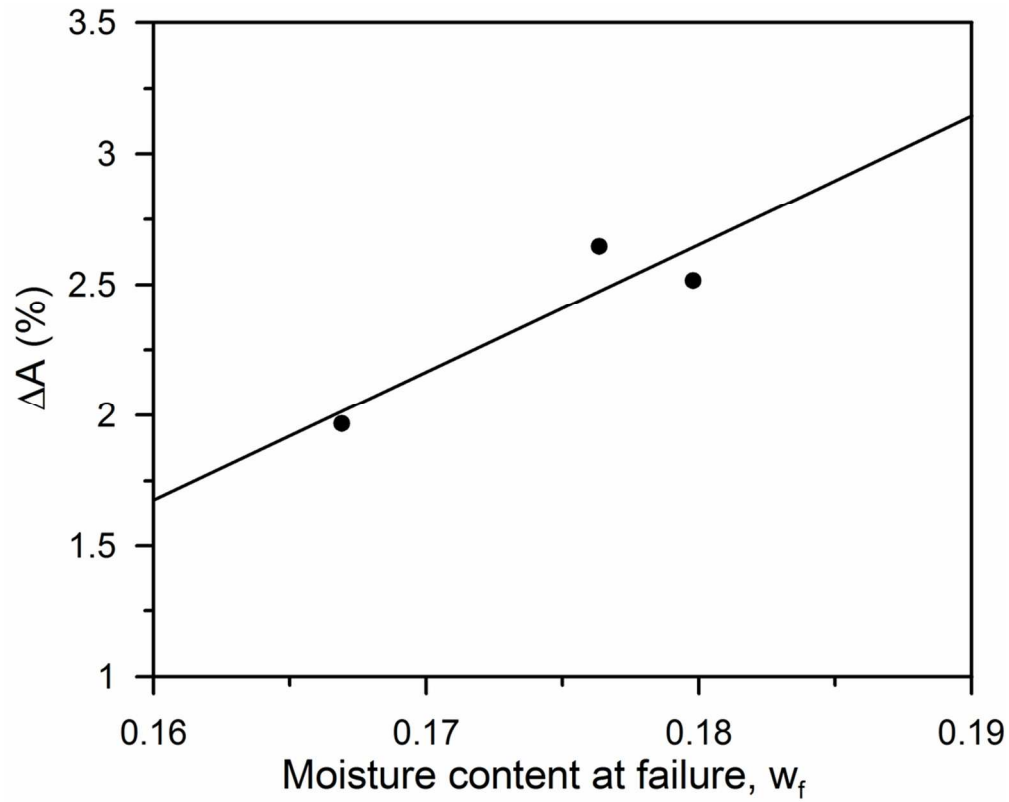


Figure 8 Method for area correction for uniaxial tension test

97x78mm (300 x 300 DPI)

1
2
3
4
5
6
7
8
9
10
11
12
13
14
15
16
17
18
19
20
21
22
23
24
25
26
27
28
29
30
31
32
33
34
35
36
37
38
39
40
41
42
43
44
45
46
47
48
49
50
51
52
53
54
55
56
57
58
59
60

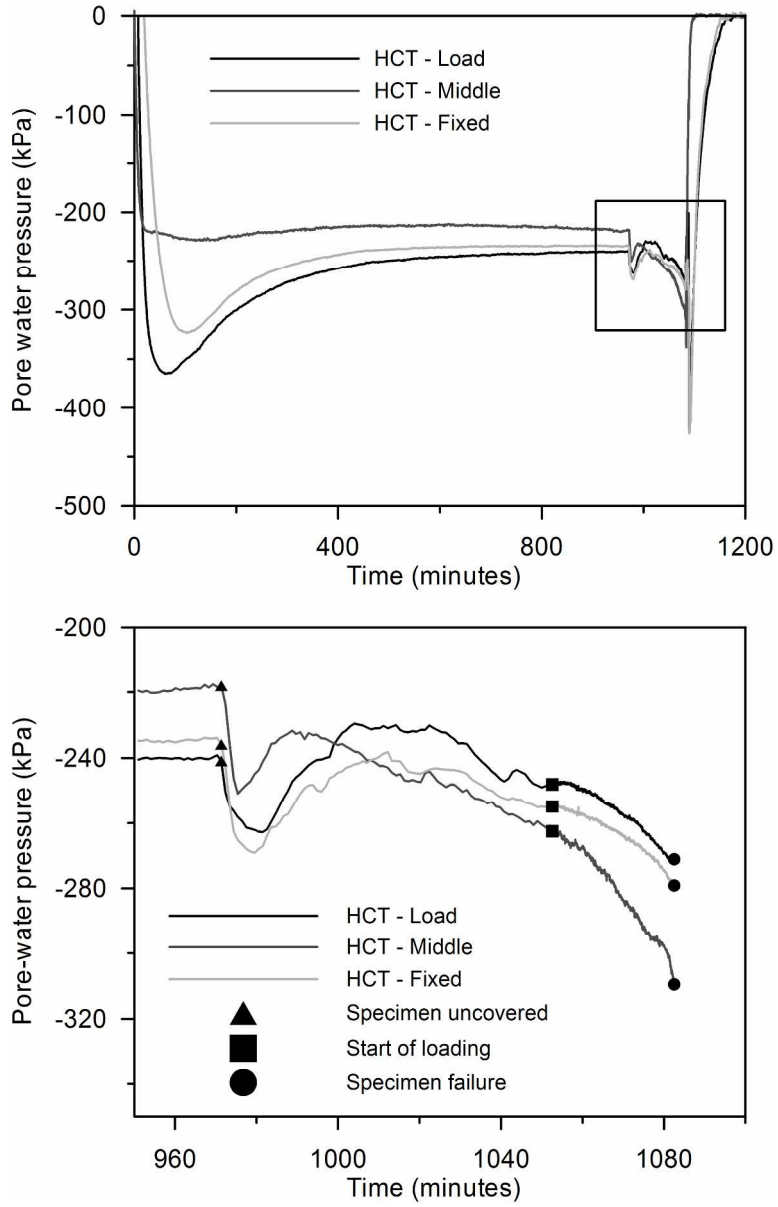


Figure 9 Evolution of pre-water pressure recorded by the tensiometers in uniaxial tensile test

196x306mm (300 x 300 DPI)

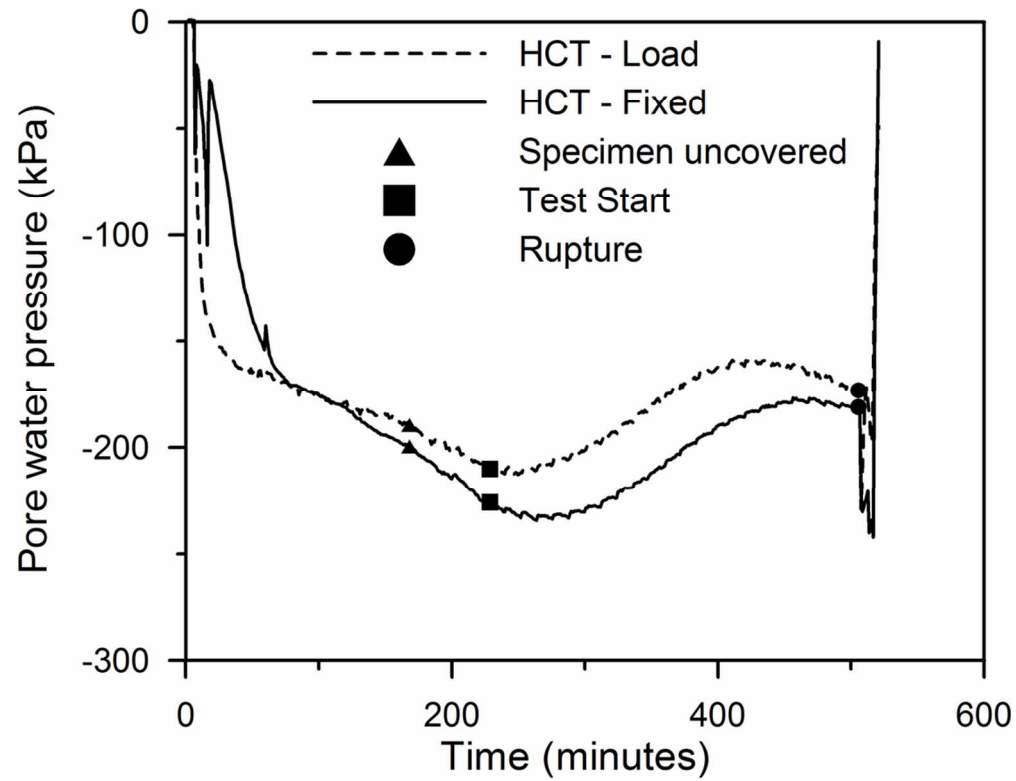


Figure 10 Evolution of pore-water pressure recorded by the tensiometers in the uniaxial compression test

97x75mm (300 x 300 DPI)

1
2
3
4
5
6
7
8
9
10
11
12
13
14
15
16
17
18
19
20
21
22
23
24
25
26
27
28
29
30
31
32
33
34
35
36
37
38
39
40
41
42
43
44
45
46
47
48
49
50
51
52
53
54
55
56
57
58
59
60

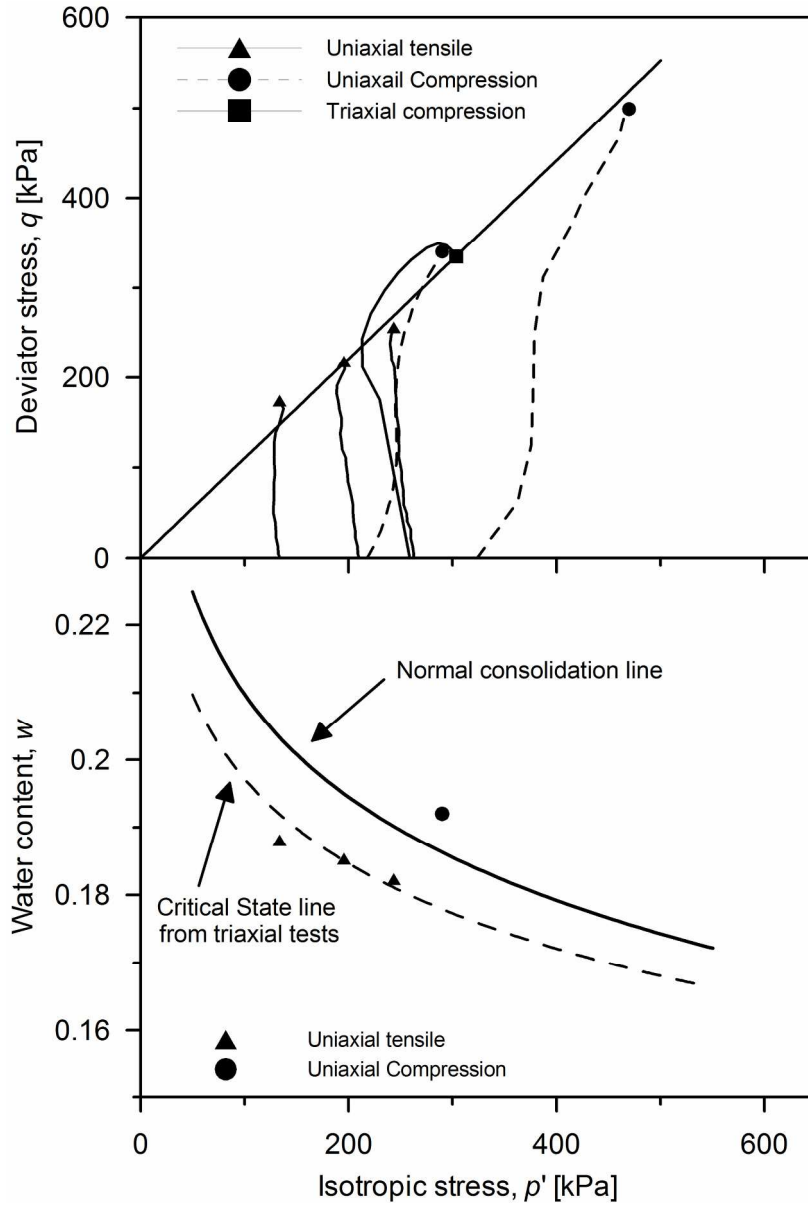


Figure 11 Critical state for uniaxial tension, uniaxial compression and triaxial compression test

177x263mm (300 x 300 DPI)

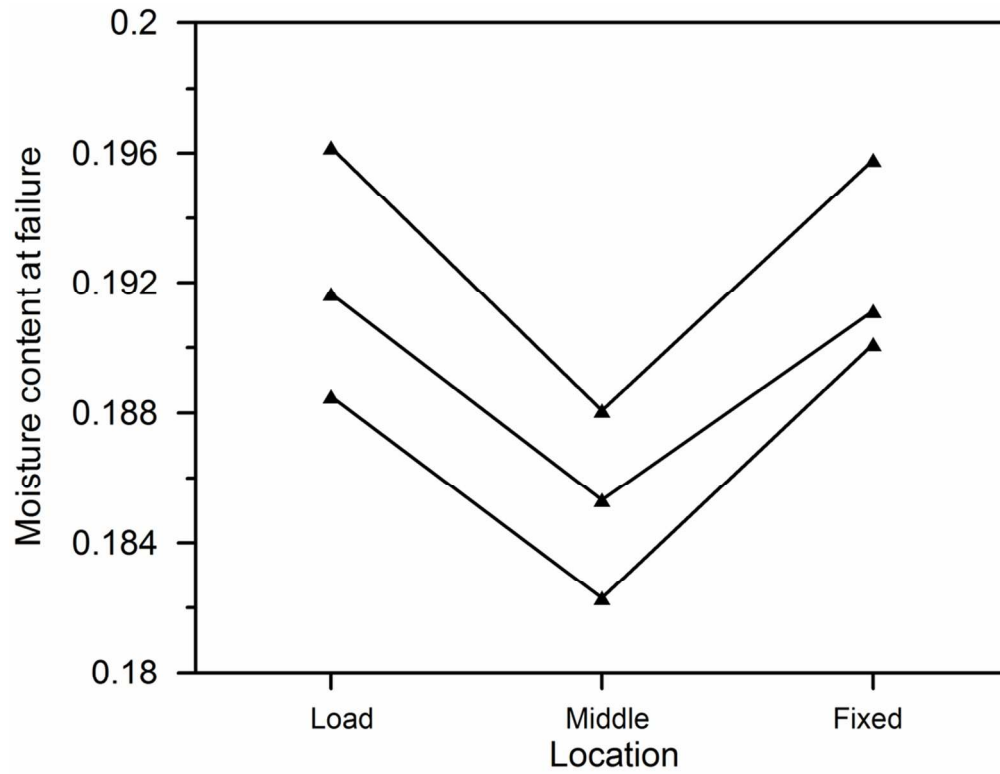
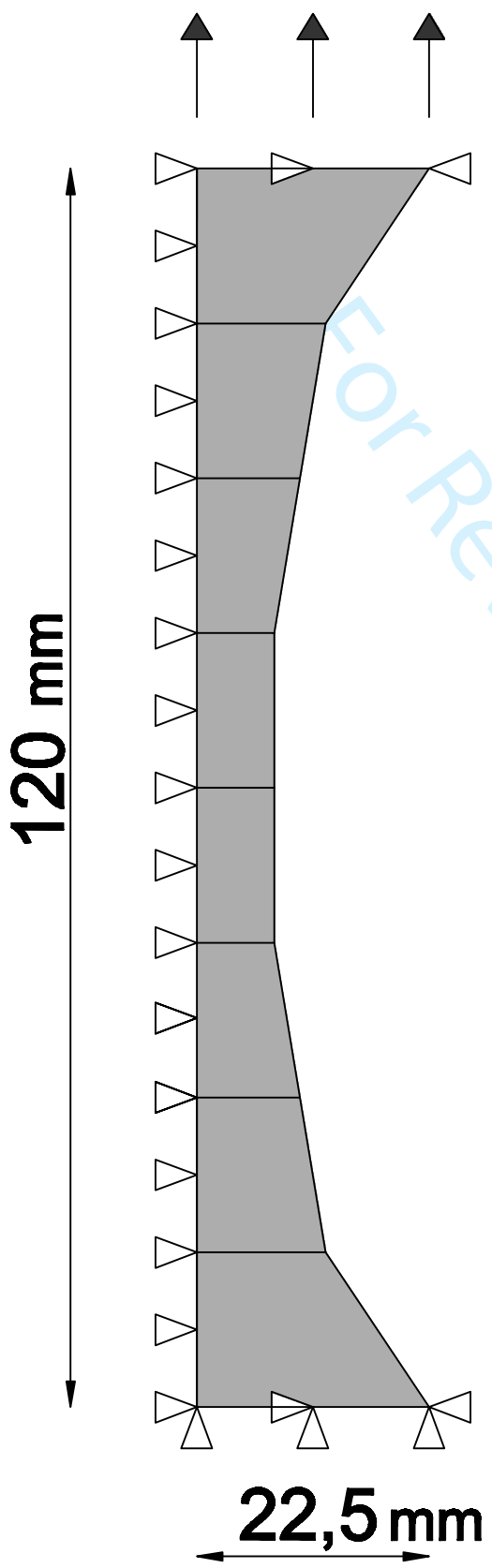


Figure 12 Moisture content at different specimen locations at failure for uniaxial tension tests

94x72mm (300 x 300 DPI)

1
2
3
4
5
6
7
8
9
10
11
12
13
14
15
16
17
18
19
20
21
22
23
24
25
26
27
28
29
30
31
32
33
34
35
36
37
38
39
40
41
42
43
44
45
46
47
48
49
50
51
52
53
54
55
56
57
58
59
60



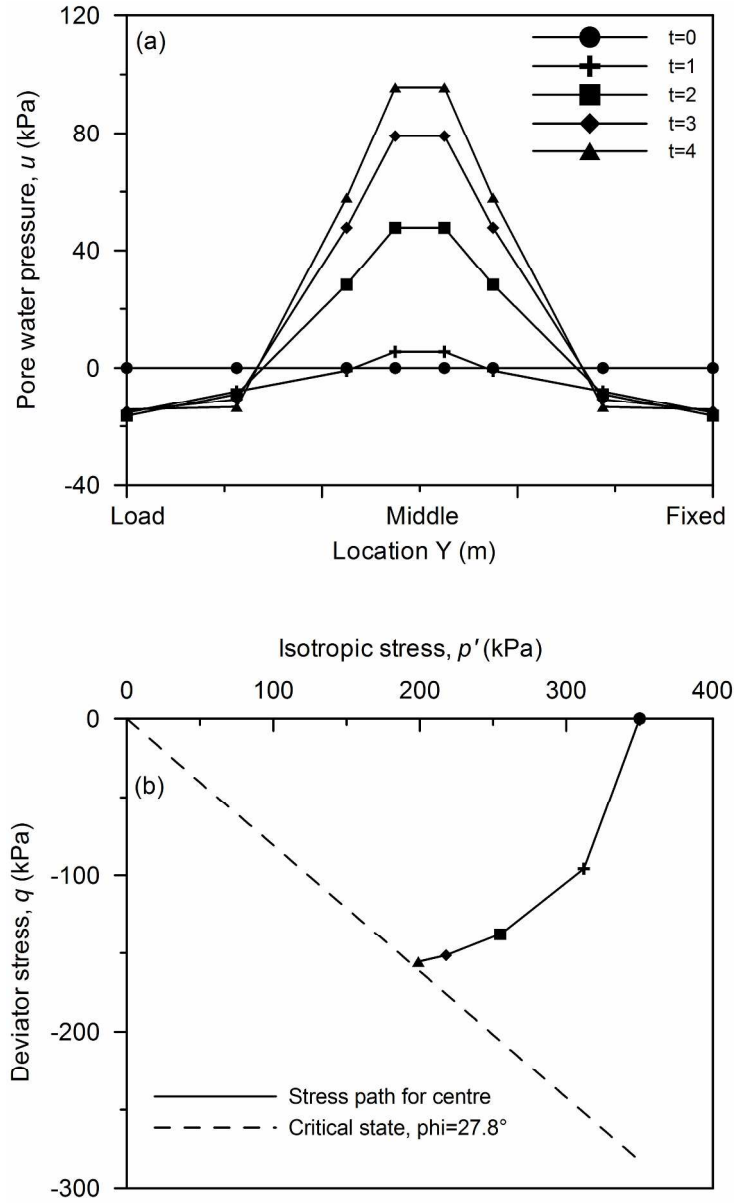


Figure 14 Results of uniaxial test simulation. (a) evolution of pore-water pressure with time. (b) stress path in the p' - q plane

204x337mm (300 x 300 DPI)